Journal of Sustainable Development of Energy, Water and Environment Systems

http://www.sdewes.org/jsdewes

Year 2018, Volume 6, Issue 4, pp 710-724

Impact of Climate Change on the Backup Infrastructure of Highly Renewable Electricity Systems

Smail Kozarcanin*[1], Gorm B. Andresen[2], Martin Greiner[3]

[1]Department of Engineering, Aarhus University, Inge Lehmanns Gade 10, Aarhus, Denmark
e-mail: sko@eng.au.dk

[2]Department of Engineering, Aarhus University, Inge Lehmanns Gade 10, Aarhus, Denmark
e-mail: gba@eng.au.dk

[3]Department of Engineering, Aarhus University, Inge Lehmanns Gade 10, Aarhus, Denmark
e-mail: greiner@eng.au.dk

Cite as: Kozarcanin, S., Andresen, G. B., Greiner, M., Impact of climate change on the backup infrastructure of highly renewable electricity systems, J. sustain. dev. energy water environ. syst., 6(4), pp 710-724, 2018,
DOI: https://doi.org/10.13044/j.sdewes.d6.0209

ABSTRACT

The global climate is currently undergoing vast changes due to the high concentrations of carbon dioxide within the atmosphere. This is already evident through the occurrence of more extreme weather events around the globe. Consequently, in this work the impact of climate change on highly weather dependent electricity systems is assessed by quantifying the extreme needs for dispatchable energy. Large-scale weather data with 3 hourly resolution, from the EURO-CORDEX project are used, reflecting three different projections of the Intergovernmental Panel on Climate Change of possible climate outcomes for the 21st century. It is found that the end-of-century period projected by two representative concentration pathways, RCP2.6 and RCP4.5, slightly increases the need for dispatchable backup energy. On the other hand, the RCP8.5 emission scenario leads to more significant increases. The demand for dispatchable energy happens to occur temporally highly clustered which introduce challenges to the electricity systems. Energy storage may be applied to handle the extreme electricity demands. To investigate this possibility, a simple theoretical modelling of energy storage is presented.

KEYWORDS

Renewable electricity systems, Climate change, Extreme events, Representative climate projections, EURO-CORDEX, HIRHAM5, ICHEC-EC-EARTH.

INTRODUCTION

The global climate is already at present time experiencing vast changes, which are leading to more extreme weather conditions. In explaining these changes, several studies point towards the emission of greenhouse gases as the reason. During the past 30 years, the global average surface temperature has increased by approximately 0.2 degrees per decade. Hansen *et al.* [1] project this to increase further with a similar rate during the first half of this century.

Nowadays, multiple studies focus on the impact of climate change on the eco and human systems. On the other hand, relatively few studies are concerned with the impact

* Corresponding author

of climate change on future sustainable energy systems. In this work, we focus on large scale electricity systems and investigate their susceptibility towards climate change, by using the latest release of climate projections provided by the Intergovernmental Panel on Climate Change (IPCC) [2]. The adapted weather driven electricity system was introduced by Rodriguez *et al.* [3] and spans a network of 30 nodes, each representing a country of Europe. These are connected by 50 links, as shown in Figure 1. The supply side to the electricity system consists of 3 hourly wind and solar power production time series for each node. These were produced by using weather data from the EURO-CORDEX project [4]. The demand side consists of 3 hourly electricity consumption time series for each node, provided by ENTSO-E [5].

Figure 1. Overview of the simplified European electric network used in this work

In this work we concentrate on climate variables that are important for the wind and solar power production. In climate modelling a clear trend is observed for these variables. In general, an increase in the wind power potential over North Europe is observed with a decreasing trend towards Southern Europe. The opposite is evident for the solar power potential. This is described in detail below. The majority of the research presented below is based on vastly different climate models. Climate models are very often a coupling of different atmospheric and oceanic models, with different underlying physics and different spatial and temporal resolutions. Consequently, biases might occur in the prediction of climate variables.

Tobin *et al.* [6] use 10 regional climate models, downscaling 6 global climate models under the SRES A1B emission scenario for the European domain and find negligible changes in the future wind projections during the end-of-century period. Exceptions are observed for the Mediterranean area for which a decrease in the wind power is projected. An identical result has been found by Bloom *et al.* [7] when using the regional climate model PRECIS over the East Mediterranean with the SRES A2 emission scenario. Aligned with this result, Hueging *et al*. [8] present similar findings in a research based on the 20C and A1B emission scenarios. For the Baltic Sea area a projected increase in the wind speeds is observed [6, 7]. A similar finding is presented by Barstad *et al.* [9] in a study based on the present and future offshore wind potentials in northern Europe by using the SRES A1B emission scenario. Similar South-North splits of the wind power potential are found by Tobin *et al.* [10] by using the RCP4.5 and RCP8.5 emission scenarios and by Carvalho *et al.* [11] by using CMIP5 climate models. Koch *et al.* [12] present negligible trends in the wind power generation over Germany by using the

RCP2.6 and RCP8.5 emission scenarios during 2031-2060. McColl *et al.* [13] evaluate the future wind projections over the UK by using the SRES A1B scenario and find slight variations in the wind speeds. Similar results are found by Seljom *et al.* [14] for a case-study of Norway based on 10 climate experiments towards the mid-century. For a study of Croatia, Pasicko *et al.* [15] find that the wind speeds increase more than 50% along the coast line during the end of the this century based on the global climate model ECHAM5-MPIOM. For a study on an aggregated EU27 by using SRES A1B and E1 emission scenarios, Dowling [16] shows a slight increase in wind power production until mid-century. For a wind dominated European energy system, increasing needs for conventional energy and storage are found in most of the Central, North and North-West areas at the end of the 21st century by Weber *et al.* [17] when using the RCP8.5 emission scenario. In addition, a more homogeneous wind power distribution is found by Wohland *et al.* [18] for the same climate projection. Hdidouan *et al.* [19] present negligible changes in the levelised cost of electricity within in the RCP8.5 emission scenario.

The Photovoltaic (PV) power generation is projected to decrease in North Europe while a slight increase is projected towards Southern Europe by Jerez *et al.* [20] when using the RCP4.5 and RCP8.5 emission scenarios. A detailed study performed by Burnett *et al.* [21] on the UK show increasing solar availability for the South and South-West regions while the Northern part will experiences a decrease. Solar PV power generation in Croatia is expected to stay unchanged [15]. For an aggregated EU27 an increase is found for the solar PV generation [16].

Highly renewable energy and electricity systems will experience states of energy deficit in which the renewable energy supply is not sufficient to cover the energy demand. Consequently, the systems need to balance the deficit by using dispatchable power, herein denoted as backup energy. It is expected that the different levels of carbon dioxide emissions implemented into the IPCC emission scenarios would affect the need for backup infrastructure. This paper is focused on the electricity system sustainability by observing the temporal occurrence of the extreme backup generation events, their magnitude and possible clustering. The main factor in the occurrence of extreme events is explained by the synergy between electricity demand and the renewable power production as hours with high demand and low power production leads to a higher likelihood of extreme backup events.

The remainder of this paper is structured as follows: The section titled “Climate scenarios” gives a brief introduction to IPCCs future climate projections: RCP2.6, RCP4.5 and RCP8.5. “Data validation” describes briefly how the data validation process is conducted. “Methodology” describes shortly the governing equations of the energy system and the approach in this work. “Results” describes the main results found during this study. “Conclusion and outlook” summarise the findings of this work and changes that may be addressed in future work.

CLIMATE SCENARIOS

Gridded data on climate variables was provided by the Danish Meteorological Institute (DMI) and consist of a 0.11° × 0.11° grid (approximately 12 km × 12 km over Europe) with 3 hourly temporal resolution. The data emanates from the regional climate model HIRHAM5 [22] downscaling the global climate model ICHEC-EC-EARTH [23] under the forcing of three different Representative greenhouse gas Concentration Pathways (RCP), each with different climate mitigations. Hereby, we include a broad range of climatic outcomes into our study. The family of RCPs consist of RCP2.6 [24], RCP4.5 [25] and RCP8.5 [26] each spanning the years 2006 to 2100. A historical period, spanning the years 1951 to 2006, serves as a reference scenario. Figure 2 shows the CO_2 emissions, atmospheric CO_2 concentrations and the radiative forcing levels that are evident from the RCP scenarios.

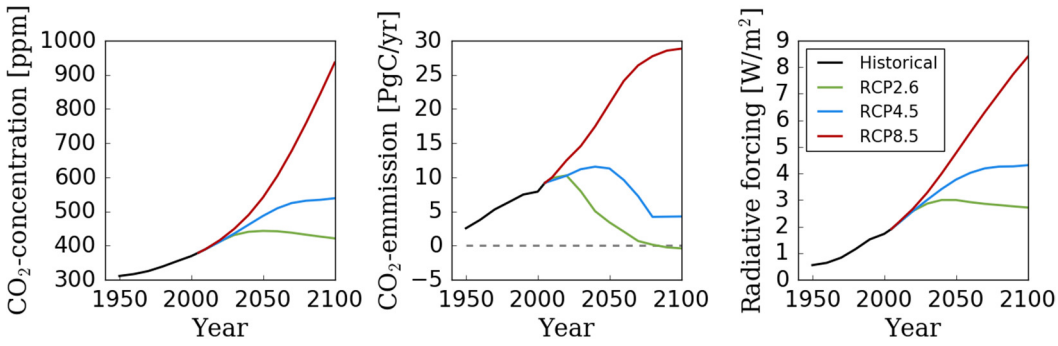

Figure 2. From left, atmospheric CO_2-concentration in ppm, CO_2-emission in PgC/yr and radiative forcing levels in W/m^2 as a function of time (black, green, blue and red colours represent the historical, RCP2.6, RCP4.5 and RCP8.5 scenarios, respectively)

RCP2.6 forms the basis of the Paris Agreement [27] to establish the goal of keeping the global average temperature increase below 2 °C at the end of the 21st century. For this to succeed the future needs to require, e.g., a decline in use of oil, a world population of 9 billion by the year 2100, increased use of cropland due to bio-energy production with a more intensive animal husbandry. Consequently, a reduction of CO_2 emissions will begin at the year 2020 and eventually negative emissions will be forced by the end of this century. The atmospheric concentration of CO_2 reduces from a value of approximately 450 ppm to slightly above 400 ppm during the second half of this century. The radiative forcing levels have to reduce during the second half of this century from a value of 3.0 W/m^2 to 2.6 W/m^2.

RCP4.5 is a scenario with stringent climate policies. To decrease the atmospheric CO_2 concentration strong reforestation programs and a decreased use of crop and grassland are assumed. These assumptions along with others lead to a reduction of CO_2 emissions starting mid-century and reaching a constant level at the year of 2080. The rate of CO_2 concentration increases heavily during the first half of this century where after it decreases reaching a level slightly above 500 ppm. The radiative forcing follows the same trend and reaching a level of 4.5 W/m^2 by the year of 2100.

RCP8.5 is a highly intensive climate scenario without climate mitigations. The main assumptions build on a world population of 12 billion by the end of the century and consequently increased use of crop and grasslands would be necessary. The CO_2 emissions are constantly increasing and reach three times the present value at the end of the century. The atmospheric concentration of CO_2 and radiative forcing levels are increasing heavily reaching values of 950 ppm and 8.5 W/m^2, respectively. Unlike the other two scenarios, RCP8.5 does not reach steady atmospheric conditions at the end of the 21st century, but it does assume that CO_2 emissions are steady at this point.

DATA VALIDATION

This section serves to describe the data conversion and validation procedure in short. A full description of these methods is provided by Kozarcanin *et al.* [28].

Wind data validation

In order to be consistent with the present day installation of wind capacities, an equivalent amount of wind turbines of the type SIEMENS SWT 107 3,600 kW have been positioned at grid points that are closest to their real world locations [29]. The 10 meter wind speeds provided by the DMI have been extrapolated to meet the wind speeds at a height of 90 meters corresponding to the hub height of the chosen turbine. The vertical extrapolation of the wind velocity (v), as a function of the height (h) above the ground is conducted by a logarithmic scaling law [30] depending on the 10 meter wind speeds and

the surface roughness length z_0 provided by the DMI. The theoretical positioning of wind turbines leads to several turbines being positioned in the same grid cell. Essentially, turbines assigned to the same grid cell may not experience the same wind conditions, wakes may occur or some turbines may be out of order due to maintenance. To take all of these effects into consideration a Gaussian kernel has been applied to the corresponding SIEMENS SWT 107 kW wind power curve before the wind speed to wind power conversion [31]. Hereafter, the grid cells have been aggregated to one time series for each country. The aggregated country-wise wind power time series have been validated according already biased wind power data obtained from www.renewables.ninja [32].

Solar data validation

The conversion of solar influx to solar PV power generation data has been performed by using the Renewable Energy atlas (REatlas), pioneered at Aarhus University [31]. This model allows for positioning of solar PV panels and choosing their orientation as desired. One solar PV panel is placed in each grid cell with azimuth angles picked from a Gaussian distribution with standard deviation $\sigma = 40$ and mean $\mu = 0$ and tilts from a Gaussian distribution with standard deviation $\sigma = 15$ and mean $\mu = 25$. The random gathering of the azimuth angle and tilt represents the real world orientations at best. For this conversion, data on the temperature, upwelling and down welling shortwave radiation was provided by DMI. The country-wise aggregated solar power production time series is validated according to biased country-wise solar data provided in www.renewables.ninja [33].

Electricity demand

The actual electric demand time series spans the years 2010 to 2015 and is provided by ENTSO-E [5]. In order to reach the desired years this time series was detrended and concatenated in order to meet the requirements.

METHODS

Each country of Europe is treated as a separate unit within the electricity network and referred to as a node (n). The wind and solar power generation time series $[W_n(t)]$ and $[S_n(t)]$, form the basis of the total renewable electricity generation $[G_n^{\mathrm{R}}(t)]$, for each node and time step (t). The electricity consumption time series $[L_n(t)]$, serves as the electrical load in the electricity system. When combined, they form the generation-load mismatch:

$$\Delta_n(t) = G_n^{\mathrm{R}}(t) - L_n(t) \tag{1}$$

which states the three-hourly difference in the total renewable energy generation and the load. This mismatch must be balanced by dispatchable energy generation or curtailment of renewable energy $[B_n(t)]$ and by energy exchange between the individual nodes $[P_n(t)]$, by means of transmission cables. Thus, the generation-load mismatch can also be written as:

$$\Delta_n(t) = B_n(t) + P_n(t) \tag{2}$$

which has to be fulfilled at all time steps by all nodes. Above, the renewable energy generation, is defined as:

$$G_n^{\mathrm{R}}(t) = \gamma_n[\alpha_n W_n(t) + (1 - \alpha_n) S_n(t)] \tag{3}$$

where the wind share of the renewable electricity generation is:

$$\alpha_n = \frac{\langle W_n \rangle_t}{\langle G_n^{\mathrm{R}} \rangle_t} \tag{4}$$

and the renewable penetration is:

$$\gamma_n = \frac{\langle G_n^{\mathrm{R}} \rangle_t}{\langle L_n \rangle_t} \tag{5}$$

By using α_n and γ_n it is possible to produce renewable power generation time series with different weights of wind and solar power. Furthermore, it is also possible to control the magnitude of the total generation of renewable electricity.

The analysis in this work is conducted by using the European aggregated backup energy generation which is given as:

$$G_{\mathrm{EU}}^{\mathrm{B}}(t) = \sum_n - \min[B_n(t), 0] \tag{6}$$

This quantity can be interpreted as the total hourly power generation from dispatchable power plants in Europe.

Transmission scheme

The unconstrained transmission scheme used in this paper assumes that all nodes are connected by power lines sufficiently large to allow the flows required to efficiently exchange the required renewable and backup energy. Furthermore, both the nodal sum of the balancing energy $[G_{\mathrm{EU}}^{\mathrm{B}}(t)]$ and the maximum required backup energy capacity $[\kappa_{\mathrm{EU}}^{\mathrm{B}}]$, is minimized for each time step. This approach forces each node to provide the same balancing relative to their mean load after the exports and imports have been processed. This approach was first introduced by Rodriguez *et al.* [3].

The required backup capacity ($\kappa_{\mathrm{EU}}^{\mathrm{B}}$), defines the amount of backup energy that the system can produce at any given time. Going by the maximum value will cause an over estimation of the required capacity as the events leading to these extremes are rare. For this reason, a high quantile (q) of the backup energy probability distribution is chosen in order to investigate the need for backup capacity as:

$$q = \int_0^{\kappa_{\mathrm{EU}}^{\mathrm{B}}} p_{\mathrm{EU}}\left(G_{\mathrm{EU}}^{\mathrm{B}}\right) dG_{\mathrm{EU}}^{\mathrm{B}} \tag{7}$$

Here, p_{EU} is the probability density function of $G_{\mathrm{EU}}^{\mathrm{B}}$.

Approach in this work

In this work we define a historical and an end-of-century period. These span the years 1970-1990 and 2080-2100, respectively.

To ensure the same amount of installed wind and solar capacities (K_n^{W}) and (K_n^{S}), in each scenario, the installed capacities during the historical period are defined as:

$$K_{n,\mathrm{hist}}^{\mathrm{W}} = \frac{\gamma_{n,\mathrm{hist}} \alpha_{n,\mathrm{hist}} \langle L_{n,\mathrm{hist}} \rangle}{CF_{n,\mathrm{hist}}^{\mathrm{W}}} \quad \text{and} \quad K_{n,\mathrm{hist}}^{\mathrm{S}} = \frac{\gamma_{n,\mathrm{hist}} (1 - \alpha_{n,\mathrm{hist}}) \langle L_{n,\mathrm{hist}} \rangle}{CF_{n,\mathrm{hist}}^{\mathrm{S}}} \tag{8}$$

$\alpha_{n,\mathrm{hist}}$ and $\gamma_{n,\mathrm{hist}}$ are fixed to 0.8 and 1, respectively, as these values minimize the need for backup infrastructure which is found by Heide *et al.* [34]. CF_n^{W} and CF_n^{S} denote the

wind and solar capacity factors. The future wind and solar generation time series is then calculated as:

$$G^{\mathrm{W}}_{n,\mathrm{scen}}(t) = K^{\mathrm{W}}_{n,\mathrm{hist}} \times CF^{\mathrm{W}}_{n,\mathrm{scen}}(t) \text{ and } G^{\mathrm{S}}_{n,\mathrm{scen}}(t) = K^{\mathrm{S}}_{n,\mathrm{hist}} \times CF^{\mathrm{S}}_{n,\mathrm{hist}}(t) \tag{9}$$

with this convention the new values for the wind share parameter and renewable penetration can be determined as:

$$\alpha_n = \frac{\langle G^{\mathrm{W}}_{n,\mathrm{scen}} \rangle}{\langle G^{\mathrm{W}}_{n,\mathrm{scen}} \rangle + \langle G^{\mathrm{S}}_{n,\mathrm{scen}} \rangle} \quad \text{and} \quad \gamma_n = \frac{\langle G^{\mathrm{W}}_{n,\mathrm{scen}} \rangle + \langle G^{\mathrm{S}}_{n,\mathrm{scen}} \rangle}{\langle L_{n,\mathrm{scen}} \rangle} \tag{10}$$

RESULTS

Table 1 presents the mean of the country-wise wind share, renewable penetration and the installed capacities during the end-of-century periods for the different emission scenarios. The wind share stays almost unchanged throughout the ensemble of emission scenarios. In contrast, the renewable penetration decreases significantly. This implies that with the present installed wind and solar capacities, on average less energy demand will be covered by renewable energy in the future scenarios. The decrease of renewable penetration is also evident from the decreased wind and solar capacity factors. A first indication on the impact of climate change on renewable energy sources show that on average the current installed capacities will eventually become less productive.

Table 1. Country aggregated mean values for $\alpha_n, \gamma_n, CF^{\mathrm{W}}_n$ and CF^{S}_n for the different scenarios

Variable	Historical	RCP2.6	RCP4.5	RCP8.5
$\langle \alpha_n \rangle_n$	0.800	0.799	0.802	0.800
$\langle \gamma_n \rangle_n$	1.00	0.979	0.983	0.965
$\langle CF^{\mathrm{W}}_n \rangle_n$	0.242	0.237	0.238	0.233
$\langle CF^{\mathrm{S}}_n \rangle_n$	0.129	0.127	0.125	0.124

Figure 3 shows the probability distributions of the backup power normalized to the average European electricity consumption. The mean and variance of the backup generation time series are shown in Table 2. Compared to the historical data, the three climate scenarios produce a higher mean and variance. RCP8.5 introduces the highest values of the mean and variance followed by the respective values for the RCP2.6 and RCP4.5 scenarios. This result implies that the RCP8.5 scenario leads to the most and strongest extreme backup events. Extreme events within the 99%-99.9% quantile are shown in Figure 4. By fitting to the tails, it is possible to study the size and occurrence of the most extreme events.

The Generalized Extreme Value (GEV) probability function is used for fits on the 99%-99.9% quantile range introduced by Reiss *et al.* [35]:

$$F_{\xi,\mu,\sigma}(x) = \exp\left\{-\left[1 + \xi \frac{(x-\mu)}{\sigma}\right]^{-1/\xi}\right\} \text{ for } 1 + \xi \frac{(x-\mu)}{\sigma} > 0 \text{ and } \xi \neq 0 \tag{11}$$

The GEV fitting parameters are the location parameter (μ), the shape parameter (ξ) and the scale parameter (σ). They are presented in Table 3. Among the fitting parameters, the focus is aligned towards the location parameter as this presents the maximum value of the GEV fit. It is observed that the location parameter increases at the end of the century. This indicates that the end of century periods introduce more and higher extreme events.

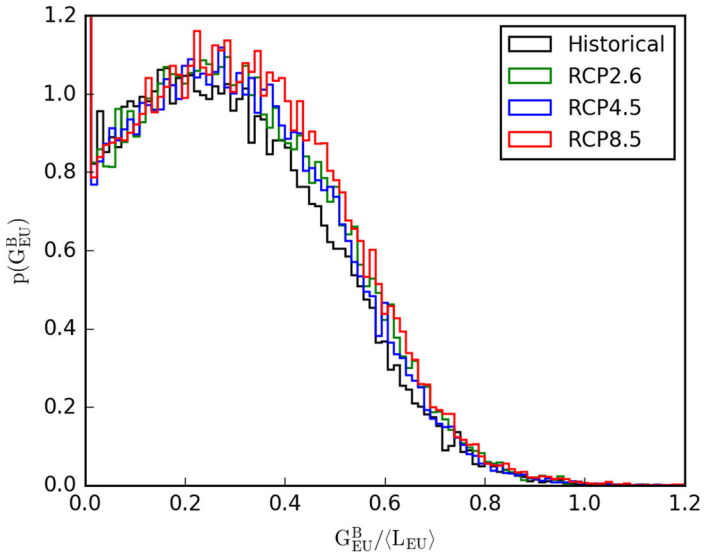

Figure 3. Probability distributions of the aggregated European backup energy based on the unconstrained transmission scheme (black, green, blue and red colours represent the historical, RCP2.6, RCP4.5 and RCP8.5 scenarios, respectively)

Table 2. Mean and variance of the backup generation time series for the ensemble of emission scenarios

	Historical	RCP2.6	RCP4.5	RCP8.5
Mean	0.164	0.184	0.178	0.195
Variance	0.042	0.046	0.044	0.048

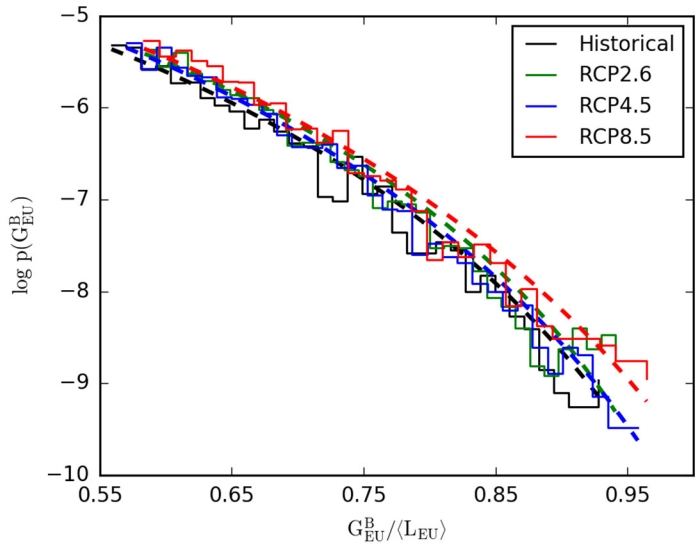

Figure 4. Probability distributions of the backup energy for the unconstrained transmission scheme (black, green, blue and red colours represent the historical, RCP2.6, RCP4.5 and RCP8.5 scenarios, respectively), dashed plots show the GEV fit

Table 3. GEV fitting parameters for the different scenarios, μ is the location parameter, σ is the scale parameter and ξ is the shape parameter

	μ	σ	ξ
Historical	0.9277	−1.088	−0.2172
RCP2.6	0.9408	−1.152	−0.2396
RCP4.5	0.9579	−1.094	−0.2060
RCP8.5	0.9646	−1.036	−0.1999

Thus far, the analysis shows that the extreme backup events are enhanced for all future climate scenarios. Information on the temporal occurrence of the extreme backup events are as well of vital importance as these challenge the energy system to a high degree. One way of determining the temporal occurrence of the extreme events is through the non-served energy defined as the required backup energy above a given backup capacity as:

$$G_{\mathrm{EN}}^{\mathrm{NS}}(t) = \max\left[G_{\mathrm{EU}}^{\mathrm{B}}(t) - \kappa_{\mathrm{EU}}^{\mathrm{B}}, 0 \middle| G_{\mathrm{EU}}^{\mathrm{B}}(t) > \kappa_{\mathrm{EU}}^{\mathrm{B}}\right] \tag{12}$$

The not-fully-served hours and the time averaged non-served backup energy $[G_{\mathrm{EN}}^{\mathrm{NS}}(t)]$ are shown in Figures 5 and 6, respectively, as a function of varying backup capacities. The not-fully-served hours are defined as the amount of not-fully-served backup energy events. From Figure 5 it is evident that all future scenarios introduce additional hours of not-fully-served backup events compared to the historical period, whereby a lack in climate mitigations of the RCP8.5 scenario leads to the highest amount. The magnitude of the non-served backup energy follows a similar trend as seen in Figure 6. To investigate how the not-fully-served events tend to cluster temporally, it is necessary to evaluate the non-served backup energy over a chosen time interval (Δt), defined as:

$$E_{\mathrm{EU}}^{\mathrm{NS}}(t, \Delta t) = \int_{t}^{t+\Delta t} \max\left[G_{\mathrm{EU}}^{\mathrm{B}}(t') - \kappa_{\mathrm{EU}}^{\mathrm{B}}, 0\right] dt' \middle| G_{\mathrm{EU}}^{\mathrm{B}}(t) > \kappa_{\mathrm{EU}}^{\mathrm{B}} \tag{13}$$

where Δt is a number varying from 0 to the total number of simulated hours. This conditional integral sums all non-served backup energy in the chosen time interval if the condition is obeyed. To detect clustering this integral has to be applied to the original backup generation time series $[G_{\mathrm{EU}}^{\mathrm{B}}(t)]$. For reference, a randomized time series is produced $[G_{\mathrm{EU}}^{\mathrm{B,rand}}(t)]$, which is based on the original time series. If the extreme events tend to distribute themselves temporally random, the non-served energy would be similar for the two cases of evaluation. On the other hand if the extreme events tend to cluster themselves one would expect the non-served energy to evolve differently as a function of Δt.

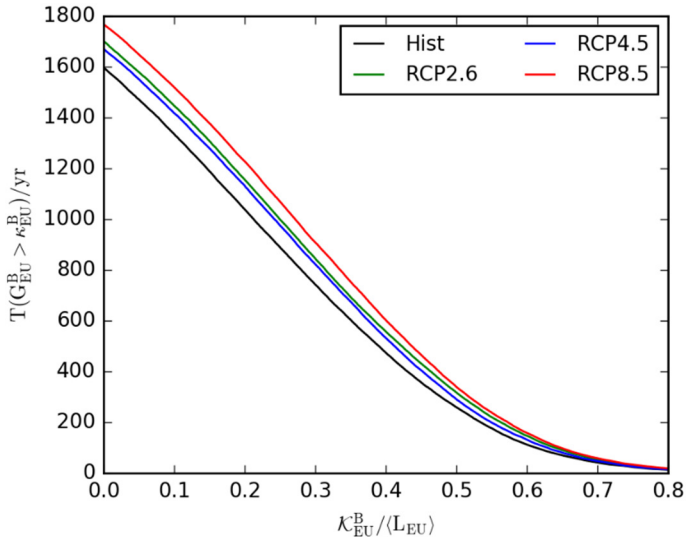

Figure 5. Not-fully-served hours of backup energy events as a function of varying backup capacities for the unconstrained transmission scheme (black, green, blue and red colors represent the historical, RCP2.6, RCP4.5 and RCP8.5 scenarios, respectively)

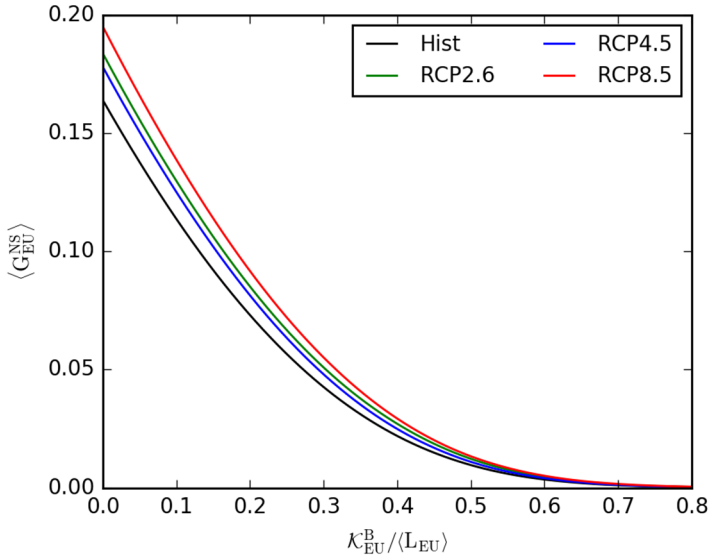

Figure 6. Time average of the total European non-served backup energy as a function of varying backup capacities for the unconstrained transmission scheme (black, green, blue and red colors represent the historical, RCP2.6, RCP4.5 and RCP8.5 scenarios, respectively)

Figures 7 and 8 show the non-served backup energy as a function of Δt for $\frac{\kappa_{EU}^{B}}{\langle L_{EU} \rangle} = 0.5$ and $\frac{\kappa_{EU}^{B}}{\langle L_{EU} \rangle} = 0.75$. $\frac{\kappa_{EU}^{B}}{\langle L_{EU} \rangle} = 0.75$ corresponds approximately to the 99% quantile of the backup generation. When using the randomized backup generation time series, the non-served backup energy reaches its asymptotic limit during the simulated hours. When evaluated for the original time series, fluctuations are observed during the simulated hours. This finding implies that the not-fully-served events occur clustered. The non-served energy show higher values for $\frac{\kappa_{EU}^{B}}{\langle L_{EU} \rangle} = 0.5$ compared to $\frac{\kappa_{EU}^{B}}{\langle L_{EU} \rangle} = 0.75$. This is evident, since less not-fully-served events occur for higher values of the available backup capacity. For $\frac{\kappa_{EU}^{B}}{\langle L_{EU} \rangle} = 0.75$ the RCP8.5 scenario shows the highest degree of clustering, in contrast to the historical period and the RCP2.6 and RCP4.5 scenarios.

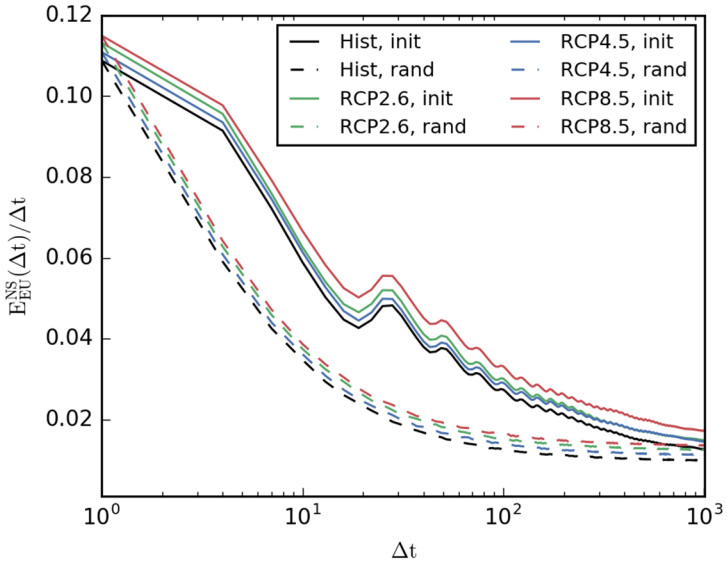

Figure 7. Non-served backup energy as a function of the time span Δt for the original time series (full drawn plots) $[G_{EU}^{B}(t)]$, and the randomized time series (dashed drawn plots) $[G_{EU}^{B,rand}(t)]$, for $\kappa_{EU}^{B}/\langle L_{EU} \rangle = 0.50$ for the unconstrained transmission scheme

Several techniques exist to take care of the not-fully-served backup events as, e.g., load shifting or storage. Storage can be very useful in taking care of single extreme events but tends to become expensive for extreme event clustering. The required amount of storage is investigated with a simple model as:

$$S_n(t) = \min\{S_n^{\max}, S_n(t-1) + [\kappa_{\mathrm{EU}}^{\mathrm{B}} - G_{\mathrm{EU}}^{\mathrm{B}}(t)]\} \tag{14}$$

where $S_n^{\max}$ is the maximum available storage capacity and $S_n(t-1)$ is the amount of storage used at time $t-1$. Figure 9 shows an example of the use of storage for the historical period as a function of time for $\frac{\kappa_{\mathrm{EU}}^{\mathrm{B}}}{\langle L_{\mathrm{EU}} \rangle} = 0.75$. The inserted plot zooms into a winter week with very low renewable power production. It is clear that when the backup energy exceeds the maximum backup capacity, in this case 75% of the European average load, the not-fully-served backup events are covered by storage. Figure 10 and Table 4 summarize the 99.9% occurrence of the storage events. The smallest mean is observed for the RCP8.5 scenario. This is caused by high storage needs. All future scenarios result in smaller mean values which indicate in higher storage needs. The variance for all scenarios are small and comparable. The amount of storage occurrences are increasing for the future climate scenarios.

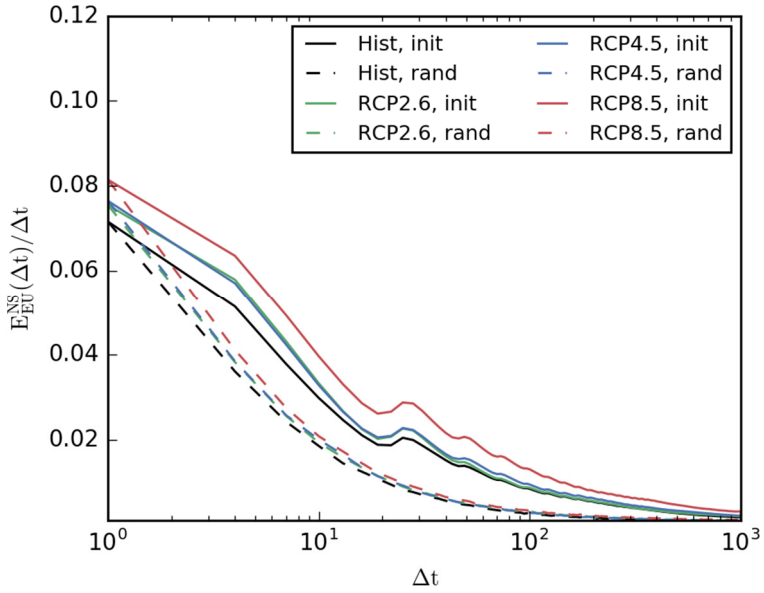

Figure 8. Non-served backup energy as a function of the time span Δt for the original time series (full drawn plots) $[G_{\mathrm{EU}}^{\mathrm{B}}(t)]$, and the randomized time series (dashed drawn plots), $[G_{\mathrm{EU}}^{\mathrm{B,rand}}(t)]$, for $\kappa_{\mathrm{EU}}^{\mathrm{B}}/\langle L_{\mathrm{EU}} \rangle = 0.75$ for the unconstrained transmission scheme

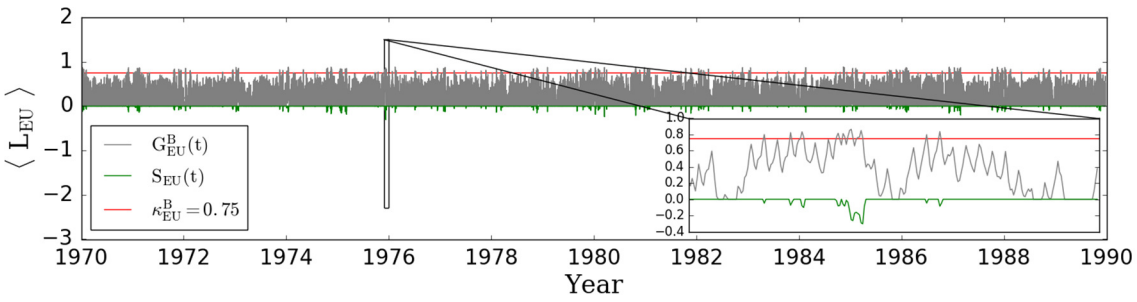

Figure 9. Backup energy and storage as a function of time ranging from 1970-1990 for a maximum backup capacity of 0.75

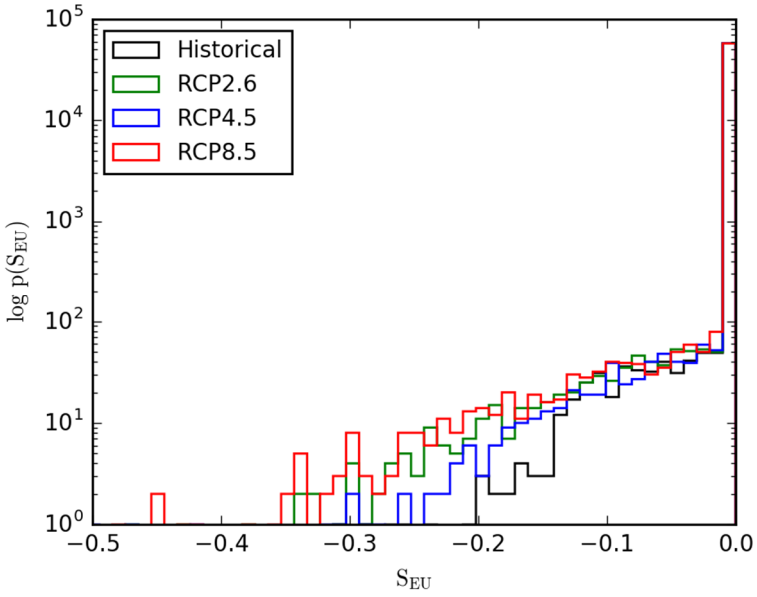

Figure 10. Logarithmic plot of the probability distributions for the 99.9% of storage events $[S_{\mathrm{EU}}(t)]$ (black, green, blue and red colours represent the historical, RCP2.6, RCP4.5 and RCP8.5 scenarios, respectively)

Table 4. Mean, variance and counts of the storage events without zero values

	Historical	RCP2.6	RCP4.5	RCP8.5
Mean	−0.065	−0.086	−0.074	−0.108
Variance	0.002	0.005	0.004	0.016
Counts	503	683	579	799

CONCLUSIONS

This paper focuses on the impact of climate change on future 100% renewable electricity systems. Each country is supplied by a wind and solar power generation time series and an electricity consumption time series. The latest release of IPCCs family of emission scenarios, RCPs, are used to represent a broad outcome of future climatic conditions. Data on climate variables was provided by the DMI, extracted from their regional climate model HIRHAM5 downscaling the global climate model ICHEC-EC-EARTH.

It is found that climate change reduces the power production of the currently installed wind and solar capacities. This reduction is most prominent within the RCP8.5 scenario, followed by reductions within the RCP2.6 and RCP4.5 scenarios. As a consequence, the need for conventional power would increase in order to cover the electricity demand. In addition, the electricity demand would get more extreme, challenging in turn the electricity system. The RCP8.5 scenario is affected at most due to missing climate mitigations. Stringent climate policies within the RCP2.6 and RCP4.5 scenario lead to less affected wind and solar sources. Also, the need for dispatchable power occurs highly clustered within the RCP8.5 scenario. The clustered events would introduce greater challenges to the electricity systems and energy storage may be applied to cover the extreme demands. A simple theoretical modelling of energy storage is presented in order to investigate this possibility. RCP2.6 and RCP4.5 are slightly affected by climate change and small differences are observed compared to the historical period. Even though climate change affects the electricity systems, the effect is small in an absolute sense and future work should address trading schemes that reduces the need for dispatchable power.

In this work, a clear yet relatively small impact of climate change on the supply side of the electricity system is observed. A natural extension is to correct the electricity consumption for impacts from electrified heating and cooling as these may be strongly affected by the temperature increase in the emission scenarios. Apart from the electricity sector it is encouraged to couple to the heating sector to form a more comprehensive energy system. Former studies show that the demand side impacts on the energy systems are stronger than the supply side impacts [16]. A study focused on Norway showed that the heating and cooling demand will decrease and increase, respectively [14]. Climate change does not lead to the same weather impacts across Europe and energy systems consisting of finer networks will bring changes to the results found in this work. The magnitude of extreme events found in this work may be enhanced if data with a higher temporal resolution are used and stronger effects on the supply side of the energy system may be observed.

ACKNOWLEDGEMENT

The authors would like to thank Ole B. Christensen and Frederik Boberg from the Danish Meteorological Institute for providing high-resolution climate data from their regional climate model HIRHAM5. SK is partially funded by the Aarhus University Research Foundation (grant AUFF-E-2015-FLS-7-26) and the READY project financed by the EU's Research and Innovation funding program FP7 (https://ec.europa.eu/research/fp7/index_en.cfm). GBA is partially funded by the READY project and the RE-Invest project, which is supported by Innovation Fund Denmark (6154-00022B). MG is partially funded by RE-INVEST as well.

REFERENCES

1. Hansen, J., Sato, M., Ruedy, R., Lo, K., Lea, D. W. and Medina-Elizade, M., Global Temperature change, *Proceedings of the National Academy of Sciences*, Vol. 103, No. 39, pp 14288-14293, September 26, 2006, https://doi.org/10.1073/pnas.0606291103
2. Intergovernal Panel on Climate Change (IPCC), http://www.ipcc.ch/, [Accessed: 22-March-2018]
3. Rodriguez, R. A., Becker, S., Andresen, G. B., Heide, D. and Greiner, M., Transmission needs across a fully renewable European Power System, *Renewable Energy*, Vol. 63, pp 467-476, 2014, https://doi.org/10.1016/j.renene.2013.10.005
4. Jacob, D., Petersen, J., Eggert, B., Alias, A., Bøssing Christensen, O., Bouwer, L. M., Braun, A., Colette, A., Déqué, M., Georgievski, G., Georgopoulou, E., Gobiet, A., Menut, L., Nikulin, G., Haensler, A., Hempelmann, N., Jones, C., Keuler, K., Kovats, S., Kröner, N., Kotlarski, S., Kriegsmann, A., Martin, E., van Meijgaard, E., Moseley, C., Pfeifer, S., Preuschmann, S., Radermacher, C., Radtke, K., Rechid, D., Rounsevell, M., Samuelsson, P., Somot, S., Soussana, J.-F., Teichmann, C., Valentini, R., Vautard, R., Weber, B. and Yiou, P., EURO-CORDEX: New High-resolution Climate change Projections for European impact research, *Regional Environmental Change*, Vol. 14, No. 2, pp 563-578, 2014, https://doi.org/10.1007/s10113-013-0499-2
5. ENTSO-E, https://www.entsoe.eu/Pages/default.aspx, [Accessed: 22-March-2018]
6. Tobin, I., Assessing climate change impacts on European Wind Energy from ENSEMBLES high-resolution Climate Projections, *Climatic Change*, Vol. 128, No. 1-2, pp 99-112, 2015, https://doi.org/10.1007/s10584-014-1291-0
7. Bloom, A., Kotroni, V. and Lagouvardos, K., Climate change impact of Wind Energy availability in the Eastern Mediterranean using the Regional Climate Model PRECIS, *Natural Hazards and Earth System Sciences*, Vol. 8, No. 6, pp 1249-1257, 2008, https://doi.org/10.5194/nhess-8-1249-2008

8. Hueging, H., Haas, R., Born, K., Jacob, D. and Pinto, J. G., Regional changes in Wind Energy Potential over Europe using Regional Climate Model ensemble Projections, *Journal of Applied Meteorology and Climatology*, Vol. 52, No. 4, pp 903-917, 2013, https://doi.org/10.1175/JAMC-D-12-086.1
9. Barstad, I., Sorteberg, A. and Mesquita, M. d.-S., Present and future Offshore Wind Power Potential in Northern Europe based on downscaled Global Climate runs with adjusted SST and Sea Ice Cover, *Renewable Energy*, Vol. 44, pp 398-405, 2012, https://doi.org/10.1016/j.renene.2012.02.008
10. Tobin, I., Jerez, S., Vautard, R., Thais, F., van Meijgaard, E., Prein, A., Déqué, M., Kotlarski, S., Fox Maule, C., Nikulin, G., Noël, T. and Teichmann, C., Climate change impacts on the Power Generation Potential of a European Mid-century Wind Farms Scenario, *Environmental Research Letters*, Vol. 11, No. 3, p 034013, 2016, https://doi.org/10.1088/1748-9326/11/3/034013
11. Carvalho, D., Rocha, A., Gómez-Gesteira, M. and Santos, C. S., Potential impacts of Climate change on European Wind Energy Resource under the CMIP5 future Climate projections, *Renewable Energy*, Vol. 101, pp 29-40, 2017, https://doi.org/10.1016/j.renene.2016.08.036
12. Koch, H., Vögele, S., Hattermann, F. F. and Huang, S., The impact of Climate change and variability on the Generation of Electrical Power, *Meteorologische Zeitschrift,* Vol. 24, No. 2, pp 173-188, 2015, https://doi.org/10.1127/metz/2015/0530
13. McColl, L., Palin, E. J., Thornton, H. E., Sexton, D. M., Betts, R. and Mylne, K., Assessing the Potential impact of Climate change on the UK's Electricity Network, *Climatic Change,* Vol. 115, No. 3-4, pp 821-835, 2012, https://doi.org/10.1007/s10584-012-0469-6
14. Seljom, P., Rosenberg, E., Fidje, A., Haugen, J. E., Meir, M., Rekstad, J. and Jarlset, T., Modelling the Effects of Climate change on the Energy System – A Case Study of Norway, *Energy Policy*, Vol. 39, No. 11, pp 7310-7321, 2011, https://doi.org/10.1016/j.enpol.2011.08.054
15. Pašičko, R., Branković, Č. and Šimić, Z., Assessment of Climate change impacts on Energy Generation from renewable Sources in Croatia, *Renewable Energy*, Vol. 46, pp 224-231, 2012, https://doi.org/10.1016/j.renene.2012.03.029
16. Dowling, P., The impact of Climate change on the European Energy System, *Energy Policy*, Vol. 60, pp 406-417, 2013, https://doi.org/10.1016/j.enpol.2013.05.093
17. Weber, J., Wohland, J., Reyers, M., Moemken, J., Hoppe, C., Pinto, J. G. and Witthaut, D., Impact of Climate change on Backup Energy and Storage needs in Wind-dominated Power Systems in Europe, arXiv preprint arXiv:1711.05569, 2017.
18. Wohland, J., Reyers, M., Weber, J. and Witthaut, D., More homogeneous Wind conditions under strong Climate change decrease the Potential for Inter-state balancing of Electricity in Europe, *Earth System Dynamics*, Vol. 8, No. 4, p 1047, 2017, https://doi.org/10.5194/esd-8-1047-2017
19. Hdidouan, D. and Staffell, I., The impact of Climate change on the levelised cost of Wind Energy, *Renewable Energy*, Vol. 101, pp 575-592, 2017, https://doi.org/10.1016/j.renene.2016.09.003
20. Jerez, S., Tobin, I., Vautard, R., Montávez, J. P., López-Romero, J. M., Thais, F., Bartok, B., Christensen, O. B., Colette, A. and Déqué, M., The impact of Climate change on Photovoltaic Power Generation in Europe, *Nature Communications*, Vol. 6, p 10014, 2015, https://doi.org/10.1038/ncomms10014
21. Burnett, D., Barbour, E. and Harrison, G. P., The UK Solar Energy Resource and the impact of Climate change, *Renewable Energy*, Vol. 71, pp 333-343, 2014, https://doi.org/10.1016/j.renene.2014.05.034
22. Bøssing Christensen, O., Drews, M., Hesselbjerg Christensen, J., Dethloff, K., Ketelsen, K., Hebestadt, I. and Rinke, A., The HIRHAM Regional Climate Model,

Version 5 (beta), Danish Climate Centre, Danish Meteorological Institute, Copenhagen, Denmark, 2007.
23. Hazeleger, W., Wang, X., Severijns, C., Ştefănescu, S., Bintanja, R., Sterl, A., Wyser, K., Semmler, T., Yang, S. and Van den Hurk, B., EC-Earth V2.2: Description and Validation of a new seamless Earth System prediction Model, *Climate Dynamics*, Vol. 39, No. 11, pp 2611-2629, 2012, https://doi.org/10.1007/s00382-011-1228-5
24. Vuuren, D. P., Stehfest, E., Elzen, M. G., Kram, T., Vliet, J., Deetman, S., Isaac, M., Goldewijk, K. K., Hof, A. and Beltran, A. M., RCP2.6: Exploring the possibility to keep Global mean Temperature increase below 2 C, *Climatic Change*, Vol. 109, No. 1-2, pp 95-116, 2011, https://doi.org/10.1007/s10584-011-0152-3
25. Thomson, A. M., Calvin, K. V., Smith, S. J., Kyle, G. P., Volke, A., Patel, P., Delgado-Arias, S., Bond-Lamberty, B., Wise, M. A. and Clarke, L. E., RCP4.5: A Pathway for stabilization of radiative forcing by 2100, *Climatic Change*, Vol. 109, No. 1-2, p 77, 2011, https://doi.org/10.1007/s10584-011-0151-4
26. Riahi, K., Rao, S., Krey, V., Cho, C., Chirkov, V., Fischer, G., Kindermann, G., Nakicenovic, N. and Rafaj, P., RCP 8.5 – A Scenario of comparatively high Greenhouse Gas Emissions, *Climatic Change*, Vol. 109, No. 1-2, p 33, 2011, https://doi.org/10.1007/s10584-011-0149-y
27. Proposal by the President, Adoption of the Paris Agreement, 2015.
28. Kozarcanin, S. and Andresen, G. B., Climate change impacts on large-scale Electricity System design decisions for the 21st Century, arXiv:1805.01364, 2018.
29. Wind Power Database, http://www.thewindpower.net/, [Accessed: 22-March-2018]
30. Tennekes, H., The Logarithmic Wind Profile, *Journal of the Atmospheric Sciences*, Vol. 30, No. 2, pp 234-238, 1973, https://doi.org/10.1175/1520-0469(1973)030<0234:TLWP>2.0.CO;2
31. Andresen, G. B., Søndergaard, A. A. and Greiner, M., Validation of Danish Wind Time series from a new Global Renewable Energy Atlas for Energy System analysis, *Energy*, Vol. 93, Part 1, pp 1074-1088, 2015, https://doi.org/10.1016/j.energy.2015.09.071
32. Staffell, I. and Pfenninger, S., Using Bias-corrected reanalysis to simulate Current and Future Wind Power output, *Energy*, Vol. 114, pp 1224-1239, 2016, https://doi.org/10.1016/j.energy.2016.08.068
33. Pfenninger, S. and Staffell, I., Long-term patterns of European PV output using 30 years of validated hourly reanalysis and Satellite Data, *Energy*, Vol. 114, pp 1251-1265, 2016, https://doi.org/10.1016/j.energy.2016.08.060
34. Heide, D., Greiner, M., Von Bremen, L. and Hoffmann, C., Reduced Storage and balancing needs in a fully renewable European Power System with excess Wind and Solar Power generation, *Renewable Energy*, Vol. 36, No. 9, pp 2515-2523, 2011, https://doi.org/10.1016/j.renene.2011.02.009
35. Reiss, R.-D., Thomas, M. and Reiss, R., *Statistical Analysis of Extreme Values*, Springer, Berlin, Germany, 2007.

Paper submitted: 09.01.2018
Paper revised: 22.03.2018
Paper accepted: 26.03.2018